Extreme lowering of deglacial seawater radiocarbon recorded by both epifaunal and infaunal benthic foraminifera in a wood-dated sediment core

Authors: Patrick A. Rafter[1]*, Juan-Carlos Herguera[2], and John R. Southon[1]

Affiliations:
[1]Department of Earth System Science, University of California, Irvine, CA, USA
[2]Centro de Investigación Cientifica y Educación Superior de Ensenada

*Correspondence to: prafter@uci.edu

Key Points
Carbon Cycle
Climate
Ice ages

Abstract:
For over a decade, oceanographers have debated the interpretation and reliability of sediment microfossil records indicating extremely low seawater radiocarbon (^{14}C) during the last deglaciation—observations that suggest a major disruption in marine carbon cycling coincident with rising atmospheric CO_2 concentrations. Possible flaws in these records include poor age model controls, utilization of mixed, infaunal foraminifera species, and bioturbation. We have addressed these concerns using a glacial-interglacial record of epifaunal benthic foraminifera ^{14}C on an ideal sedimentary age model (wood calibrated to atmosphere ^{14}C). Our results affirm—with important caveats—the fidelity of these microfossil archives and confirm previous observations of highly depleted seawater ^{14}C at intermediate depths in the deglacial northeast Pacific.

1.0 Introduction

Given modern carbon cycle perturbations (Keeling, 1960), it is critical to understand the drivers of natural atmospheric carbon dioxide (CO_2) variability. A prime example of this 'natural' atmospheric CO_2 variability is the increase that occurs at the end of each late-Pleistocene ice age (Figure 1) (Petit et al., 1999). The ocean's ability to store and release CO_2 makes it a likely driver of past changes in this important greenhouse gas (Broecker, 1982).

A valuable tool in the effort to characterize the marine carbon cycle over the most recent of these intervals is the ^{14}C content of benthic and planktic foraminifera tests (Broecker et al., 1988), which are assumed to reflect the ^{14}C content of dissolved inorganic carbon (DIC) in the waters in which they grew. This tracer provides a geochemical "clock" with a predictable decay but ^{14}C is also affected by a variety of other processes, including the time since the water mass exchanged CO_2 with the atmosphere, the degree of this exchange, variations in the atmospheric

concentration of ^{14}C at the time of exchange (Figure 1), as well as the contribution of ^{14}C-depleted carbon via mixing and / or other carbon sources (e.g., seafloor volcanism (Ronge et al., 2016)).

We can relate seawater ^{14}C content to modern ocean conditions by using delta notation or $\Delta^{14}C$ (Figure 1), which corrects for ^{14}C decay:

$\Delta^{14}C = e^{(-^{14}C \text{ age}/8033)} / e^{(-\text{Calendar Age}/8267)} - 1$ (1)

(Equation (1) is multiplied by 1000 to give units of per mil [‰]. The ^{14}C age Calendar Age is given in years before 1950 or "before present" (BP).)

The available benthic foraminifera $\Delta^{14}C$ records paint a complicated picture of glacial to interglacial seawater ^{14}C content. For example, a record of benthic foraminifera $\Delta^{14}C$ from the intermediate depth subtropical eastern North Pacific (Lindsay et al., 2015; Marchitto et al., 2007) shows $\Delta^{14}C$ depleted relative to the atmosphere by >400‰ during the deglaciation (from ≈19-to-11,000 years BP; see Figure 1). Later work showed benthic foraminifera with similar or even lower $\Delta^{14}C$ values during the deglaciation in other parts of the intermediate depth ocean (≈500-1000 m), such as the 617 m deep Eastern Equatorial Pacific (Stott et al., 2009) and the 596-820 m deep Arabian Sea (Bryan et al., 2010). Given that the lowest observed modern intermediate-depth seawater $\Delta^{14}C$ is about -300‰ (or only ≈300‰ lower than the atmosphere) (Key et al., 2004), the low benthic foraminifera $\Delta^{14}C$ / old ^{14}C ages suggest much lower $\Delta^{14}C$ and older seawater DIC ^{14}C ages during the deglaciation.

A leading explanation of these low intermediate depth $\Delta^{14}C$ values involves the storage of carbon in an isolated deep-sea reservoir during the glacial period followed by the rapid flushing of this low $\Delta^{14}C$ / old ^{14}C aged carbon through the intermediate-depth ocean during the deglaciation—a deep-sea carbon flush that also explains the observed elevation of atmospheric CO_2 concentrations and lowering of atmospheric CO_2 ^{14}C content (Marchitto et al., 2007). This interpretation is qualitatively supported by observations of lower deep-sea dissolved oxygen concentrations before the deglaciation (Jaccard et al., 2016; Jaccard and Galbraith, 2011).

The ocean carbon flushing hypothesis predicts that deep-sea $\Delta^{14}C$ during the glacial period will be lower than the extreme $\Delta^{14}C$ lowering of the intermediate-depth $\Delta^{14}C$ during the deglaciation (Figure 1) because of mixing with shallower waters with higher $\Delta^{14}C$. However, while deglacial $\Delta^{14}C$ as low or lower than in Figure 1 is observed in some deep-sea waters during the glacial period (Sikes et al., 2000; Skinner et al., 2010; Keigwin and Lehman, 2015) and intermediate-depth waters (Burke and Robinson, 2012)—observations that are consistent with the flushing hypothesis—it is not clear how these low $\Delta^{14}C$ signals are not mixed away en route to the lower latitudes (Hain et al., 2011). Additionally, the lower $\Delta^{14}C$ in Figure 1 is

not observed at all intermediate depth sites during the deglaciation (De Pol-Holz et al., 2010; Rose et al., 2010). Furthermore, the extreme $\Delta^{14}C$ lowering observed in intermediate-depth benthic foraminifera during the deglaciation does not appear to be quantitatively consistent with an isolated deep-sea reservoir (Hain et al., 2011).

The inconsistency of the available $\Delta^{14}C$ records is compounded by assumptions about the reliability of the foraminifera archive as a recorder of seawater DIC ^{14}C. For example, an important assumption when using planktic foraminifera is that the depth of calcification does not vary based on modern observations (e.g., (Field, 2004)). The use of benthic foraminifera seemingly circumvents this problem, and those that live at the sediment-water interface ("epifaunal") have been demonstrated to record seawater carbon chemistry (Keigwin, 2002; Roach et al., 2013). However, the abundance of epifaunal benthic foraminifera is typically low relative to benthic species that abide within the sediment ("infaunal"). Rather than recording seawater ^{14}C content directly, the infaunal species provide a record of sediment pore water carbon chemistry, which may or may not reflect bottom water conditions.

A further complication to published benthic foraminifera $\Delta^{14}C$ observations is that both the epifaunal and infaunal species are typically rare in sediments, leading to the common use of mixed benthic species. The mixed species approach has led, in some rare cases, to anomalously low $\Delta^{14}C$ values / old ^{14}C ages by inclusion of anomalously depleted ^{14}C *Pyrgo* spp. (Magana et al., 2010)—an anomaly that may not be a global phenomenon (Thornalley et al., 2015). While mono-species epifaunal benthic foraminifera ^{14}C measurements exist (Thornalley et al., 2011, 2015; Voelker et al., 1998), we are unaware of any continuous glacial-interglacial records of mono-species epifaunal foraminifera ^{14}C content. (One study used mixed planispiral species, whose morphology predicts an epifaunal habitat (Galbraith et al., 2007).) An additional influence on benthic foraminifera $\Delta^{14}C$ is bioturbation (Keigwin and Guilderson, 2009), which is infrequently quantified, even though it can dramatically affect the observed ^{14}C age (Costa et al., 2018). The doubts raised by the above complications are amplified by converting the benthic foraminifera ^{14}C age to $\Delta^{14}C$, which requires the user to assign a calendar age to the sediment.

Finally, constraining the age model of sediment cores typically relies upon several assumptions. For example, planktic foraminifera ^{14}C is commonly used to identify the calendar age of sedimentary material, although this requires assumptions about the depth habitat of the planktic foraminifera and the 'reservoir age' of the surface waters (the offset between atmosphere and ocean ^{14}C). Other means for determining the calendar age involve tying temporal variability to other paleoclimate/paleoceanographic records (Marchitto et al., 2007; Stott et al., 2009). In rare instances, the ^{14}C of wood from terrestrial plants provides a direct recording of atmospheric ^{14}C, which is well-dated and provides an excellent sedimentary age model (Broecker, 2004; Zhao and Keigwin, 2018), although this work provides some recommendations for utilizing this technique (see below). For our understanding of

136 past and future carbon cycling processes, it is essential that we thoroughly explore
137 these influences and build confidence in these sediment proxy records.
138
139 Here, we provide a test of the fidelity of the benthic foraminifera $\Delta^{14}C$ proxy using
140 ^{14}C measurement of benthic foraminifera species from two sediment cores near the
141 mouth of the Gulf of California (white diamond in Figure 2). These sediment cores
142 are unusual in that both epifaunal and infaunal benthic foraminifera microfossils are
143 plentiful and allow us a unique opportunity to test the fidelity of the benthic
144 foraminifera $\Delta^{14}C$ proxy. The foraminiferal abundance were quantified to account
145 for bioturbation and the age model is calibrated to the well-constrained
146 atmospheric ^{14}C record (Reimer et al., 2013) via wood found alongside the
147 foraminifera. These cores (from hereon, the 'Gulf' sites) allow us to present glacial-
148 interglacial ^{14}C measurements produced from 4 benthic foraminifera, including the
149 preferred epifaunal species *Planulina ariminensis* (Keigwin, 2002). The Gulf core
150 sites are bathed in the subsurface, northward flowing Mexican Coastal Current (MCC
151 in Figure 2), which are the source of the California Undercurrent (Gómez-Valdivia et
152 al., 2015)—waters that also bathe the well known sites on the Pacific margin of Baja
153 California shown in Figure 1 (from hereon, the 'California Undercurrent' sites). This
154 shared seawater source gives the expectation of similar $\Delta^{14}C$ signal at both
155 sedimentary locations—an expectation that we exploit to examine the potential for
156 diagenetic alteration of the benthic foraminifera $\Delta^{14}C$ observations relative to
157 sedimentation rates, which are significantly lower at the Gulf sites ($\approx$2 to 5 cm kyr^{-1};
158 our study) relative to the Undercurrent sites (>25 cm kyr^{-1}; (Lindsay et al., 2015;
159 Marchitto et al., 2007)) (where 'kyr' is 1000 years). These and other hydrological,
160 geochemical, and diagenetic influences on benthic foraminifera $\Delta^{14}C$ are examined
161 below with the goal of answering an important question: are these benthic
162 foraminifera $\Delta^{14}C$ records recording an extreme lowering of seawater $\Delta^{14}C$ during
163 the deglaciation?
164
165 **2.0 Materials and Methods**
166 Sediment from Gulf of California sites LPAZ-21P (22.9°N, 109.5°W; 625 m) and
167 ET97-7T (22.9°N, 109.5°W; 640 m) (white diamond in Figure 2; Table 1) was
168 washed using de-ionized water in a 63-μm sieve. Foraminifera abundance estimates
169 of *Planulina ariminensis* (benthic; epifaunal species), *Uvigerina peregrina* (benthic;
170 shallow infaunal species), *Trifarina bradyi* (benthic; deep infaunal species), mixed
171 *Bolivina* (benthic; deep infaunal species), and *Globogerina bulloides* (planktic
172 species) were made after quantitatively dividing the >150 μm fraction of each
173 sample using a Green Geological aluminum microsplitter. These estimates were
174 made for all samples from core LPAZ-21P and select samples from core ET97-7T.
175 Preliminary work measured the ^{14}C age of mixed benthic species from the ET97-7T
176 core site and although the species abundance was not quantified, they primarily
177 included *Planulina* spp., *Uvigerina* spp., and *Trifarina* spp.
178
179 **2.1 Radiocarbon measurements**

Monospecies foraminifera and wood were selected for ^{14}C analysis from the >250 μm fraction from both Gulf sediment cores. Each foraminifera sample was sonicated in methanol (≈1 minute) to release detrital carbonates trapped within open microfossil chambers. At least 10% of each sample was dissolved using HCl to remove secondary calcite (precipitated post-deposition), though in-house tests with and without this pretreatment yielded identical results for these core sites. Wood fragments from the >250 μm fraction were prepared using standard acid-base-acid treatments.

Samples were graphitized following (Santos et al., 2007) and analyzed at the Keck Carbon Cycle Accelerator Mass Spectrometry (KCCAMS) laboratory at University of California, Irvine (Southon et al., 2004). We report radiocarbon as $\Delta^{14}C$ in units of per mil [‰] (see equation (1) above), which is corrected for decay based on its age normalized to 1950, according to convention (Stuiver and Polach, 1977). Analysis of a sedimentary standard (FIRI-C) alongside measurements indicates a combined sample preparation and measurement ^{14}C age error ranging from ±50 years for a full size sample (≈0.7 mg of C) to ±500 years for very small samples (<0.1 mg of C). Because of the similar location of the sites near the mouth of the Gulf of California, we combined the ^{14}C measurements from both cores.

2.2 Oxygen and carbon stable isotopic measurements

The $^{18}O/^{16}O$ and $^{13}C/^{12}C$ of benthic foraminifera was measured using a Kiel IV Carbonate Device coupled to a Delta XP isotope ratio mass spectrometer at the University of California, Irvine. Isotopic ratios are reported in delta notation, where: $\delta^{13}C = (^{13}C/^{12}C_{sample} / {}^{13}C/^{12}C_{standard} - 1)$ and $\delta^{18}O = (^{18}O/^{16}O_{sample} / {}^{18}O/^{16}O_{standard} -1)$. Each was multiplied by 1000 to give units of "per mil". The standard for both measurements is VPDB.

2.3 Age model construction for Gulf of California sediment cores

The age model for LPAZ-21P (between 30,000-to-12,100 years Before Physics or "BP," where BP is 1950) is constrained by 13 microscopic wood fragments calibrated to calendar ages using CALIB7.1 (Stuiver et al., 2017) with the IntCal13 atmospheric ^{14}C dataset (Reimer et al., 2013) (squares in Figure 3A and 3C). Five wood measurements from LPAZ-21P did not pass our test for use as an age model constraint (upside-down triangles in Figure 3C and see text below). All LPAZ-21P depths shallower than 63 cm are notably darker, changing from light to very dark brown over a depth interval of ≈2 cm. The onset of this change is constrained to be younger than 12,100±1,100 years BP (12.1±1.1-kyr BP) by a calibrated wood ^{14}C age (see Appendix). There was a lack of suitable wood in LPAZ-21P in Holocene-aged sediments and our age models for this interval are constrained using *U. peregrina* ^{14}C ages (circles in Figure 3A), corrected for a modern reservoir age of 1240 years based on nearby seawater DIC ^{14}C age observations at 600 m (Key et al., 2004) and converted to calendar ages using CALIB7.1 (Stuiver et al., 2017). These Holocene ^{14}C ages are not tied to foraminifera abundance maxima and hence the Holocene calendar ages should be considered preliminary. The youngest calendar

age for LPAZ-21P was 5.3-kyr BP, suggesting piston core over-penetration during sediment coring. Samples younger than the LPAZ-21P coretop were obtained from the LPAZ-21PG core, whose age model was constrained identical to the Holocene-aged sediments of LPAZ-21P (see above). The Bayesian age model program BACON (Blaauw and Christen, 2011) was used to estimate the age and model error between the age model constraints.

The ET97-7T age model is constrained in three ways: using ^{14}C ages of 5 pieces of microscopic wood from 18.9- to 15.3-kyr BP (diamonds in Figure 3A and 3C); using *U. peregrina* ^{14}C ages corrected for reservoir age in Holocene-aged sediment; and by synchronizing the apparently region-wide transition from light to dark-colored sediments (van Geen et al., 2003) to 12.1-kyr based on the wood-constrained age from LPAZ-21P ("X"s in Figure 3A and 3D). In lieu of reflectance data to quantify the brightness of the sediment cores, we present Ca/Al estimated using X-Ray Fluorescence (see Method below). The reasoning behind using Ca/Al is that this metric: (1) Normalizes changes in terrestrial Ca input by dividing by Al and (2) Is sensitive to the abundance of calcium carbonate microfossils. The sudden lowering of Ca/Al at ≈65 cm in LPAZ-21P and ≈71 cm in ET97-7T is coincident with decreased abundance of foraminifera and this presumably causes the darkening of these and other Holocene-aged sediments across the region. Ages between these constraints were estimated using BACON, as was done for the LPAZ-21P cores.

2.4 X-Ray Fluorescence

We estimated the Ca/Al of LPAZ-21P and ET97-7T using an Avaatech XRF core scanner at the Scripps Institution of Oceanography Sediment Core Repository. The archived halves of the sediment cores were lightly scraped to expose less oxidized sedimentary material before analysis. More detailed methods (including software and signal processing) are identical to those previously described in (Addison et al., 2013).

2.5 Wood ^{14}C age test

Terrestrial plant life must have a younger ^{14}C age / higher $\Delta^{14}C$ than all contemporaneous foraminifera because of the air-sea difference in ^{14}C content (e.g., see Figure 1) and we used this inherent ^{14}C age difference to check for contemporary deposition of the wood and microfossils in Gulf sediments. Fourteen out of 20 microscopic wood fragment ^{14}C ages passed the test and include one interval that may have been influenced by macrofauna consumption and excretion has a wood ^{14}C age that is younger than foraminifera (see below).

One wood measurement that spectacularly failed this test came from presumably mid-to-late-Holocene sediment (i.e., <12-kyr BP aged sediments based on the depth below seafloor). However this wood yielded a ^{14}C age of >25-kyr (see upside down triangles in Figure 3). We explain this remarkable ^{14}C age difference as the erosion and deposition of relict wood stored on land before washing to the Gulf during a rain event. The other wood measurements that failed this test gave ^{14}C ages typically within measurement error or were ≈1000 ^{14}C years older than foraminifera ^{14}C age. In total, 5 out of 20 wood ^{14}C measurements were older than foraminifera in our

sediment cores relative to 1 out of 26 wood ^{14}C measurements by the only other study with similar length age model (Zhao and Keigwin, 2018). This difference may be because faster sedimentation rate of Zhao and Keigwin, (2018) (20-60 cm kyr^{-1}) leads to less bioturbation and a faster burial of the wood alongside foraminifera microfossils. Otherwise, the difference in rejections could be explained by our measurement of all wood, whereas (Zhao and Keigwin, 2018) only measured wood that still retained bark.

In light of this unusual application of calibrated ^{14}C ages on wood in a marine setting, it is important to understand the potential errors. We assigned all calibrated wood ages a ±100 year uncertainty added in quadrature to the measurement and calibration error to account for possible lag in seafloor deposition. Note that the *asymmetry* of any errors associated with assuming contemporary growth of wood and foraminifera must be considered: if we underestimate the time from wood growth to sediment deposition, the actual calendar age of the sediment would be *younger* than the calendar age given in this study; hence foram $\Delta^{14}C$ values would be even *lower* than the large depletions shown here (see equation 1 and Results). Additionally, it is possible that a longer-than-expected time period between wood growth and sediment deposition could be "masked" by declining atmospheric ^{14}C concentrations (Figure 1), allowing the wood ^{14}C age to pass our test for inclusion in the age model. These different histories for the wood found in our sediment cores would mean the calendar age is younger than we have assumed, adjusting our benthic foraminifera $\Delta^{14}C$ values to lower values than reported below. Given these potential influences on a wood ^{14}C age-constrained age model, the uncertainty should primarily include the younger calendar age and not the ±100 year Gaussian uncertainty we assume. However, without a more exhaustive statistical study of age model errors when using wood, it is simpler and more conservative to utilize a Gaussian age model error.

Given these potential errors, it is worth considering the modern ^{14}C age difference between seawater at the sediment-water interface and the atmosphere. A measurement of seawater DIC ^{14}C age close to our core site and depth (at 22°N, 110°W at 598 m), gives a ^{14}C age of 1240 years BP. Assuming that DIC at this depth has not yet been seriously impacted by bomb ^{14}C (Key et al., 2004) this would predict a pre-bomb wood-to-benthic foraminifera ^{14}C age difference of 1240 years BP. This is consistent with our data presented below, where the ^{14}C age difference between concurrent wood and benthic foraminifera *P. ariminensis* and *U. peregrina* varies between this and even larger ^{14}C age differences (Table 2).

3.0 Results

3.1 Age model and sedimentation rates

The old coretop age for the LPAZ-21P core (5.3-kyr BP) indicates a poor recovery of the youngest sediments by the piston core, similar to nearby coring sites on the Pacific margin (van Geen et al., 2003). The LPAZ-21PG gravity core calendar ages range from 7954 to 504 years BP, suggesting that it recovered much of the material

missed by the piston core. Both cores give similar sedimentation rates of 16 to 18 cm kyr^{-1} over this Holocene interval (see Figure 3A). The nearby trigger core ET97-7T gives a slightly lower sedimentation rate for this time interval (pink in Figure 3), which may result from regional hydrographic differences, different seafloor dynamics, or sediment recovery based on different coring technology. Core recovery equipment may also explain differences in downcore sedimentation rates between the sites (5 cm kyr^{-1} versus 19 cm kyr^{-1} in ET97-7T during the 13-to-15-kyr BP interval; Figure 3).

A wood ^{14}C age-constrained age model has only been applied twice before (Broecker, 2004; Zhao and Keigwin, 2018) and it is worth quantifying the suitability of this approach in our cores. First, we applied a quantitative test: the wood ^{14}C age must be older than all coexisting foraminifera ^{14}C ages. This test included planktic foraminifera measurements that will be discussed in a following manuscript. The difference between benthic foraminifera and wood ^{14}C ages is illustrative of the effectiveness of this test. The difference between the ^{14}C age of benthic foraminifera (*P. ariminensis* and *U. peregrina*) and coexisting, wood that passed our test is 2346±1599 years (n=14) and 2309±1063 years (n=14), respectively (Table 2). Only comparing wood with foraminifera abundance maxima gives a ^{14}C age difference of 3353±1957 years (*P. ariminensis*; maximum of 5815 years, minimum of 1077 years, n=6) and 2697±1117 years (*U. peregrina*; maximum of 4145 years, minimum of 1480 years, n=6). These values are consistent with bottom water at our core sites that are near or older than the modern, pre-bomb seawater - atmosphere ^{14}C age difference of 1240 years (see above). Given these results, we argue that our test for excluding wood ^{14}C ages is appropriate, but that unlikely circumstances may have existed that could hide the timescale of deposition. In the event of a longer-than-expected time between wood growth and deposition in the sediment, the calendar age would be biased to younger ages, making benthic foraminifera $\Delta^{14}C$ values even more depleted than calculated (Figure 5).

The excellent age model controls provided by wood ^{14}C provide us with a powerful (and not always flattering) insight to the sedimentation rates of the Gulf cores. For example, our wood-constrained calendar ages identify two periods of slow sedimentation (or possibly hiatus events) in LPAZ-21P (between 22.7- to 19.5-kyr BP and 12.1- to 9-kyr BP; see grey bars in Figures 3, 4, and 6). The earlier interval is bracketed by wood-constrained calendar ages while the shallower / more recent sedimentation rate slowdown begins approximately at the end of the Younger Dryas or less than ≈12.1-kyr BP.

3.2 Foraminifera abundance estimates

The abundance of four benthic and one planktic foraminifera in the LPAZ-21P core is highly variable with the planktic species *G. bulloides* as high as >6000 g^{-1} of sediment (Figure 4). The least abundant foraminifera was *P. ariminensis*, which had peak values just over 200 g^{-1}. Abundance of *G. bulloides* and all other planktic foraminifera (not shown) in these sediments dropped sharply after 12.1-kyr BP—a loss of planktic foraminifera preservation that is also seen at the nearby California

Undercurrent site (red diamond in Figure 2) (Lindsay et al., 2015). The abundance of *P. ariminensis* also drops to zero after 12.9-kyr BP, while *U. peregrina* and *T. bradyi* decline to lower, but persistent values ≈2-kyr later. *Bolivina* spp. are known to persist in low oxygen waters and are the most abundant foraminifera in LPAZ-21P and LPAZ-21PG sediments for the past 7-kyr.

It is important to identify the abundance of sedimentary foraminifera when measuring ^{14}C because the vertical mixing of sediment by macro- and micro-fauna (bioturbation) can grossly bias the ^{14}C results (Keigwin and Guilderson, 2009) causing foraminifera ^{14}C ages to be older on the shallow side of abundance peaks, and vice versa. This effect was recently shown for Juan de Fuca Ridge sediments, where foraminifera ^{14}C measurements shallower than a large abundance maxima were biased to "old" ^{14}C ages (Costa et al., 2018). Below we explore the ^{14}C age and $\Delta^{14}C$ trends for each benthic foraminifera species.

3.3 Comparing benthic foraminifera ^{14}C measurements

Examining the differences in the ^{14}C age of the four benthic foraminifera species (Figure 5), we find a maximum 5775 year offset between *U. peregrina* and *T. bradyi* ^{14}C age (the former being older). Even though the sample sizes are small (7 to 42), comparing the preferred epifaunal *P. ariminensis* (Keigwin, 2002) to the other species suggests that: (1) *Bolivina* spp. ^{14}C age is older, (2) *T. bradyi* ^{14}C age is younger, and that (3) *U. peregrina* gives a ^{14}C age that is most similar to the epifaunal species (Table 3; left side).

The comparisons above, however, are likely influenced by bioturbation and a more appropriate examination would only compare the ^{14}C ages of foraminifera at abundance maxima where the influence of bioturbation is minimized (see above). One drawback to an abundance maximum-only comparison is that it draws from a smaller pool of observations (e.g., n=2 for the *P. ariminensis* vs. *Bolivina* spp.), which limits the significance of these statistics. This comparison suggests that—on average—*U. peregrina* (n=8) and *T. bradyi* (n=4) give similar ^{14}C ages to epifaunal species, but with a large (10±861 years) to very large (35±1125 years) range of variability. On average, *Bolivina* spp. at abundance maxima (n=2) gives an even older ^{14}C age difference from the preferred epifaunal species (Table 3; right side).

Despite the monospecies $\Delta^{14}C$ differences, the glacial-deglacial trends of all four benthic foraminifera ^{14}C (corrected for decay and shown as $\Delta^{14}C$ in Figure 5) from our cores near the mouth of the Gulf of California (the 'Gulf' sediment core sites) are depleted relative to the atmosphere during the deglaciation, but are considerably higher during the Holocene. The shallowest and therefore most recent benthic foraminifera $\Delta^{14}C$ are roughly equal to modern DIC $\Delta^{14}C$ measurements of -173‰ at the depth of the cores (Key et al., 2004). Error bars denote 1 sigma calendar age and $\Delta^{14}C$ errors and symbols represent measurements at abundance maxima. Triangles with error bars at bottom of each plot indicate the calendar ages and 1 sigma uncertainties provided by wood dates. The ^{14}C ages of foraminifera on either side of

abundance peaks can also be "corrected", although this requires an assumption about bioturbation rates, but this will be the subject of future work.

Each monospecies $\Delta^{14}C$ record in Figure 5A to D is compared with the nearby benthic foraminifera $\Delta^{14}C$ record from the open Pacific margin of Baja California (a combination of mixed and mono-species benthic foraminifera on the original age model; see core locations in Figure 2 and Table 1) (Lindsay et al., 2015; Marchitto et al., 2007). Additionally, a series of mixed benthic $\Delta^{14}C$ measurements (preliminary work on ET97-7T where species abundance was not quantified) is shown in Figure 5D. All Gulf benthic foraminifera $\Delta^{14}C$ measurements are compiled in Figure 5E (black) to illustrate the overall range of values given by the 4 benthic and mixed species measurements relative to the atmospheric (grey; (Reimer et al., 2013)) and the Undercurrent site $\Delta^{14}C$ (red). As can be seen by these multiple views of the dataset, all benthic foraminifera $\Delta^{14}C$ trends at both Gulf and Undercurrent sites shift to lower values after 20-kyr BP. These depletions relative to atmospheric $\Delta^{14}C$ are very large, but even lower $\Delta^{14}C$ values are observed for intermediate depth sediment core sites in the eastern equatorial Pacific (Stott et al., 2009).

3.4 Influence of macrofaunal consumption and excretion on sediment ^{14}C ages?

In a single interval from 106 to 110 cm of the LPAZ-21P core, which was predicted to be ≈25.5-kyr based on interpolation from our Bayesian statistical age model, the wood and benthic and planktic foraminifera ^{14}C ages were conspicuously younger than expected, giving a $\Delta^{14}C$ value well above the contemporary atmosphere (956.3‰; see circle in Figure 6). In fact, wood found within this sedimentary interval suggests a calendar age of only 19.2-kyr BP, giving a much lower *U. peregrina* $\Delta^{14}C$ of -88.6‰. This lower $\Delta^{14}C$ value is consistent with values for the wood-constrained calendar age (see square in Figure 6). If these anomalous but self-consistent observations are not simply a result of human error (mislabeling or other sampling problem) they may indicate the presence in this interval of "zoophycos" or the remnants of downward-burrowing macrofauna (as was suggested by (Lougheed et al., 2017)). By consuming and later excreting sedimentary material, these worms are able to move 'younger' sedimentary components deeper in the sediment column, though if this is the cause, the self-consistency of our ^{14}C measurements in this reworked interval (where microfossil and wood ^{14}C ages suggest an undisturbed sample) is surprising.

3.5 The stable isotopic composition of oxygen ($\delta^{18}O$) and carbon ($\delta^{13}C$)

The epifaunal benthic foraminifera (*P. ariminensis*) $\delta^{18}O$ and $\delta^{13}C$ measurements in Figure 7 uses new and published data from LPAZ-21P (Herguera et al., 2010), but on our wood-constrained age model. As previously reported, intermediate depth $\delta^{13}C$ shows little variability between the Last Glacial Maximum (LGM) and Holocene at the depth of this core (624 m; (Herguera et al., 2010)). Benthic foraminifera $\delta^{18}O$ has similar magnitude of change to benthic $\delta^{18}O$ for the nearby Undercurrent core sites (Figure 7 in (Lindsay et al., 2016)), although the Undercurrent benthic $\delta^{18}O$ increase

to Holocene values may lag the Gulf site values (compare (Lindsay et al., 2016) with Figure 7).

4.0 Discussion

Based on the work presented here, the trend towards an extreme lowering of intermediate-depth benthic foraminifera $\Delta^{14}C$ in the subtropical northeastern Pacific (the California Undercurrent site in Figures 1, 2, and 5) (Lindsay et al., 2015; Marchitto et al., 2007) cannot be explained by species biases, bioturbation, or poor age model controls (Figure 5). This statement is supported by our ^{14}C measurements of the epifaunal benthic foraminifera *P. ariminensis*—a species known to provide the best record of seawater carbon at the sediment-water interface (Keigwin, 2002)—and several commonly used infaunal benthic foraminifera from sediment cores "upstream" of the canonical record of these extreme $\Delta^{14}C$ observations (Figures 1 and 5). Our measurements indicate that even though the potential variability between infaunal and the preferred epifaunal species' ^{14}C ages is relatively large (several hundred years; Table 3), the average ^{14}C age difference at foraminifera abundance maxima is <100 years, and the overall trend towards extremely low $\Delta^{14}C$ during the deglaciation cannot be explained by bioturbation and persists regardless of species.

4.1 Comparing Gulf and Undercurrent site deglacial records

Our Gulf sediment core observations indicate that the mixed-species $\Delta^{14}C$ measurements from the Undercurrent sites shown in Figures 1 and 5 are largely accurate, although the higher values that form the middle of this 'W' shaped anomaly (from ≈15- to 13-kyr BP) are not obviously reproduced by any of the 4 mono-species benthic foraminifera $\Delta^{14}C$. It is possible that this and other some smaller-scale features of a mixed benthic $\Delta^{14}C$ record reflect the bias of a particular species and/or the influence of bioturbation in our lower sedimentation rate sites. For example, the benthic foraminifera *T. bradyi* is a possible suspect for biasing mixed benthic $\Delta^{14}C$ measurements because it is relatively large, dense, and sometimes has large deviations to younger ^{14}C ages than the other species (Figure 5). Nevertheless, the overall agreement between the independently derived Undercurrent and Gulf records lend credence to the methods used to construct the age model by Marchitto et al., (2007) and tested by Lindsay et al., (2016). We should note that we cannot explain the large offset between the records from 30-to-25-kyr BP, although this comparison only includes one observation from the Undercurrent sites.

The similar $\Delta^{14}C$ trends at both Undercurrent and Gulf sites despite sedimentation rate differences and sediment core hiatus lends additional support for the robustness of the $\Delta^{14}C$ trends (Lindsay et al., 2016) and against events such as the large-scale—and far-fetched—redeposition of sand-sized sedimentary components. In principle, the circulation of bottom waters from the Gulf to the Undercurrent sediment core sites could allow for redeposition of benthic foraminifera with much older ^{14}C ages, but a much larger reworked component (and hence much older

benthic foraminifera ^{14}C ages) would logically be expected at the "upstream" Gulf sites. In fact, sedimentary redeposition should be amplified at the lower sedimentation rate Gulf site, but significantly lower benthic foraminifera $\Delta^{14}C$ is not observed for any of the species at the Gulf sites.

These findings allow us to now focus our questions on two potential explanations for the extreme depletions of benthic foraminifera $\Delta^{14}C$ observed during the deglaciation: (1) it is a diagenetic signal imparted onto both epifaunal and infaunal foraminifera after burial or (2) it reflects a real change in seawater $\Delta^{14}C$ during the deglaciation.

4.2 Can diagenesis explain the low deglacial $\Delta^{14}C$?

Investigating the potential for diagenetic alteration of benthic foraminifera $\Delta^{14}C$, we are not concerned about the newly observed coupling between carbonate dissolution and precipitation (Subhas et al., 2017), which only involves a few monolayers of surface carbonate. Instead, producing the extreme $\Delta^{14}C$ lowering observed at Undercurrent and Gulf sites (Figure 5) and other sites around the globe (Bryan et al., 2010; Stott et al., 2009; Thornalley et al., 2011) requires the precipitation of depleted ^{14}C on or within the foraminifera test is required.

This authigenic calcium carbonate formation and foraminifera ^{14}C content has been examined in several ways. For example, benthic foraminifera from the eastern equatorial Pacific give some of the lowest observed deglacial $\Delta^{14}C$ values (-609‰), but Scanning Electron Microscope images show no authigenic carbonate on benthic or planktic foraminifera (Stott et al., 2009). Calcium carbonate overgrowth (via the conversion of $CaCO_3$ to $CaSO_4$ (gypsum)) was observed in Santa Barbara Basin sediments (Magana et al., 2010), but would not influence the ^{14}C content of the microfossil. What's more, extreme ^{14}C depletions of mixed benthic foraminifera from this and other sites were found to be biased by *Pyrgo* spp., which are inexplicably depleted in ^{14}C (Ezat et al., 2017). Other work suggests *younger-than-expected* ^{14}C ages from the precipitation of carbonate onto foraminifera tests after core recovery (Skinner et al., 2010). Cook et al., (2011) observed anomalously low foraminifera $\Delta^{14}C$, high $\delta^{18}O$, and low $\delta^{13}C$ was consistent with authigenic carbonate precipitation from methane. Wycech et al., (2016) also compared the ^{14}C ages of translucent and opaque mono-specific planktic foraminifera from the same sediment horizons and found the opaque foraminifera (thought to contain authigenic carbonate) had ^{14}C ages more than 10,000 years older than the translucent tests.

Neither the Gulf nor the Undercurrent site benthic foraminifera measurements display the telltale signs of simultaneous $\Delta^{14}C$, $\delta^{18}O$, and $\delta^{13}C$ anomalies seen by Cook et al., (2011) (see Figure 7). What's more, the planktic $\Delta^{14}C$ values from the Undercurrent site do not show anomalous depletion during the deglaciation (Lindsay et al., 2015), which is expected for post-depositional alteration / authigenic carbonate formation. It is possible that a completely different process of authigenic

carbonate formation is occurring in the subtropical eastern Pacific, but we cannot elaborate on what this mechanism might be. It is possible that authigenic carbonates are removed from the foraminiferal test during the 10% acid leaching pre-treatment at KCCAMS (see Methods), although selected pre-treatment tests did not significantly alter the ^{14}C ages. This pretreatment was not used in the Wycech et al., (2016) comparisons, but will be examined in our future studies.

Finally, given the near identical deglacial $\Delta^{14}C$ trends at the Undercurrent and Gulf sites despite very different sedimentation rates (20-30 cm kyr^{-1} at the Undercurrent versus 1-to-5 cm kyr^{-1} at the Gulf; Figure 3) it would be surprising if the same depleted $\Delta^{14}C$ trends were of diagenetic origin. This is because a faster sedimentation rate will decrease the potential for authigenic mineralization by decreasing the exposure time of the foraminifera. This reduction in exposure time would apply to both the microfossil's exposure at the sediment-water interface and at sediment depths favorable to authigenic carbonate precipitation. Thus, while the potential influence of authigenic carbonate on the primary foraminifera record is an important area of research that deserves further study, the similarity of the Undercurrent and Gulf records argues against contamination from authigenic carbonate precipitation as the major influence on these benthic foraminifera $\Delta^{14}C$ values.

5.0 Conclusions

If the extreme deglacial depletion of benthic foraminifera $\Delta^{14}C$ at these northeastern Pacific sites cannot be explained by species or habitat bias, bioturbation, or poor age model control, the remaining explanation is that they reflect a change in seawater DIC $\Delta^{14}C$. Looking to other proxy systems, deep-sea coral $\Delta^{14}C$ in the North Atlantic and Southern Ocean—archives with excellent age model control and different diagenetic influences—also display depleted deglacial $\Delta^{14}C$ during the deglaciation (Adkins et al., 1998; Burke and Robinson, 2012; Chen et al., 2015; Robinson et al., 2005). However, the deep-sea coral $\Delta^{14}C$ depletion have a different timing and are not as extreme as observed for the Gulf of California and California Undercurrent sites (Figure 5E).

A leading candidate among the potential explanations for these and other intermediate depth records (Bryan et al., 2010) is the deep-sea sequestration and flushing of carbon through the intermediate depth ocean (Basak et al., 2010; Du et al., 2018; Lindsay et al., 2016; Marchitto et al., 2007). This interpretation is plausibly consistent with ^{14}C records from only a few sites, such as the deep Southern Ocean (Barker et al., 2010; Skinner et al., 2010) and deep Nordic Seas (Thornalley et al., 2015). However, using an 18-box geochemical ocean-atmosphere model to simulate glacial-interglacial ocean circulation and carbon cycling, Hain et al., (2011) argue that matching the observed $\Delta^{14}C$ depletions in the intermediate depth, Northern Hemisphere sites requires unrealistic changes in ocean chemistry (e.g., lower surface ocean alkalinity) and ocean dynamics (i.e., mixing). Specifically, to appropriately "age" deep-sea ^{14}C requires deep-sea anoxia, which is not observed.

Furthermore, the release of this deep-sea ^{14}C to intermediate depths would dissipate much quicker than the several thousand year anomaly shown in Figure 5E.

An alternative explanation involves the addition of ^{14}C-depleted carbon via mid-ocean ridge (MOR) volcanism (Ronge et al., 2016), which is indirectly supported by evidence for increased MOR activity (Lund, 2013; Middleton et al., 2016; Tolstoy, 2015). The locations and depths of the extreme benthic foraminifera $\Delta^{14}C$ lowering are also suggestive of a MOR influence, given their proximity to the East Pacific Rise / Gulf of California (Marchitto et al., 2007; Ronge et al., 2016; Stott et al., 2009; this study), the Red Sea (Bryan et al., 2010), and Mid-Atlantic Ridge (Thornalley et al., 2011). However, this hypothesis of enhanced carbon flux from seafloor volcanism must also explain the many intermediate-depth sites that do not show anomalous deglacial $\Delta^{14}C$ depletions (Broecker & Clark, 2010; Cléroux et al., 2011; De Pol-Holz et al., 2010). Furthermore, this proposed carbon addition must have been associated with an alkalinity addition, without which the increased seawater CO_2 concentrations and therefore lower seawater pH would have caused a global-scale carbonate dissolution event (Lindsay et al., 2016; Stott and Timmermann, 2011).

In summary, our work strongly suggests that at least for the Gulf of California and adjacent Pacific sites, the foraminifera $\Delta^{14}C$ proxy records real ^{14}C changes in deglacial intermediate depth seawater DIC, but the question of what caused those changes remains open. Careful examination to confirm or disprove the fidelity of the benthic foraminifera $\Delta^{14}C$ on a case by case basis will be a critical part of building a reliable body of data to identify the controls on glacial-interglacial marine carbon cycling.

Acknowledgments: C. Bertrand, A. Hangsterfer (SIO Core Repository), H. Martinez, N. Shammas, M. Ayad, M. Rudresh, A. De la Rosa, J. Troncoso, J. DeLine, J. Sanchez, C. Manlapid, M. Chan, as well as T. Marchitto and two anonymous reviewers.

References:

Addison, J. A., Finney, B. P., Jaeger, J. M., Stoner, J. S., Norris, R. D. and Hangsterfer, A.: Integrating satellite observations and modern climate measurements with the recent sedimentary record: An example from Southeast Alaska: Modern SE Alaska Fjord Sediment Records, J. Geophys. Res. Oceans, 118(7), 3444–3461, doi:10.1002/jgrc.20243, 2013.

Adkins, J. F., Cheng, H., Boyle, E. A., Druffel, E. R. M. and Edwards, L. R.: Deep-Sea Coral Evidence for Rapid Change in Ventilation of the Deep North Atlantic 15,400 Years Ago, Science, 280, 1998.

Ahn, J. and Brook, E. J.: Siple Dome ice reveals two modes of millennial CO2 change during the last ice age, Nat. Commun., 5(1), doi:10.1038/ncomms4723, 2014.

628 Barker, S., Knorr, G., Vautravers, M. J., Diz, P. and Skinner, L. C.: Extreme deepening of
629 the Atlantic overturning circulation during deglaciation, Nat. Geosci., 3(8), 567–571,
630 doi:10.1038/ngeo921, 2010.

631 Basak, C., Martin, E. E., Horikawa, K. and Marchitto, T. M.: Southern Ocean source of
632 14C-depleted carbon in the North Pacific Ocean during the last deglaciation, Nat.
633 Geosci., 3(11), 770–773, doi:10.1038/ngeo987, 2010.

634 Blaauw, M. and Christen, J. A.: Flexible paleoclimate age-depth models using an
635 autoregressive gamma process., Bayesian Anal., 6, 457–474, 2011.

636 Broecker, W. S.: Glacial to interglacial changes in ocean chemistry, Prog. Oceanogr.,
637 11, 1982.

638 Broecker, W. S.: Ventilation of the Glacial Deep Pacific Ocean, Science, 306(5699),
639 1169–1172, doi:10.1126/science.1102293, 2004.

640 Broecker, W. S. and Clark, E.: Search for a glacial-age 14C-depleted ocean reservoir,
641 Geophys. Res. Lett., 37(13), 1–6, doi:10.1029/2010GL043969, 2010.

642 Broecker, W. S., Klas, M., Ragano-Beavan, N., Mathieu, G. and Mix, A.: Accelerator
643 mass spectrometry radiocarbon measurements on marine carbonate samples from
644 deep sea cores and sediment traps, Radiocarbon, 30(3), 35, 1988.

645 Bryan, S. P., Marchitto, T. M. and Lehman, S. J.: The release of 14C-depleted carbon
646 from the deep ocean during the last deglaciation: Evidence from the Arabian Sea,
647 Earth Planet. Sci. Lett., 298(1–2), 244–254, doi:10.1016/j.epsl.2010.08.025, 2010.

648 Burke, A. and Robinson, L.: The Southern Ocean's Role in Carbon Exchange During
649 the Last Deglaciation, Science, 335(6068), 557–561, doi:10.1126/science.1215110,
650 2012.

651 Chen, T., Robinson, L. F., Burke, A., Southon, J., Spooner, P., Morris, P. J. and Ng, H. C.:
652 Synchronous centennial abrupt events in the ocean and atmosphere during the last
653 deglaciation, Science, 349(6255), 1537–1541, doi:10.1126/science.aac6159, 2015.

654 Cléroux, C., deMenocal, P. and Guilderson, T.: Deglacial radiocarbon history of
655 tropical Atlantic thermocline waters: absence of CO2 reservoir purging signal, Quat.
656 Sci. Rev., 30(15–16), 1875–1882, doi:10.1016/j.quascirev.2011.04.015, 2011.

657 Cook, M. S., Keigwin, L. D., Birgel, D. and Hinrichs, K.-U.: Repeated pulses of vertical
658 methane flux recorded in glacial sediments from the southeast Bering Sea,
659 Paleoceanography, 26(2), n/a-n/a, doi:10.1029/2010PA001993, 2011.

660 Costa, K. M., McManus, J. F. and Anderson, R. F.: Radiocarbon and Stable Isotope
661 Evidence for Changes in Sediment Mixing in the North Pacific over the Past 30 kyr,
662 Radiocarbon, 60(01), 113–135, doi:10.1017/RDC.2017.91, 2018.

De Pol-Holz, R., Keigwin, L., Southon, J., Hebbeln, D. and Mohtadi, M.: No signature of abyssal carbon in intermediate waters off Chile during deglaciation, Nat. Geosci., 3(3), 192–195, doi:10.1038/ngeo745, 2010.

Du, J., Haley, B. A., Mix, A. C., Walczak, M. H. and Praetorius, S. K.: Flushing of the deep Pacific Ocean and the deglacial rise of atmospheric CO2 concentrations, Nat. Geosci., doi:10.1038/s41561-018-0205-6, 2018.

Ezat, M. M., Rasmussen, T. L., Thornalley, D. J. R., Olsen, J., Skinner, L. C., Hönisch, B. and Groeneveld, J.: Ventilation history of Nordic Seas overflows during the last (de)glacial period revealed by species-specific benthic foraminiferal 14C dates, Paleoceanography, 32(2), 172–181, doi:10.1002/2016PA003053, 2017.

Field, D. B.: Variability in vertical distributions of planktonic foraminifera in the California Current: Relationships to vertical ocean structure, Paleoceanography, 19(2), n/a-n/a, doi:10.1029/2003PA000970, 2004.

Galbraith, E. D., Jaccard, S. L., Pedersen, T. F., Sigman, D. M., Haug, G. H., Cook, M., Southon, J. R. and Francois, R.: Carbon dioxide release from the North Pacific abyss during the last deglaciation, Nature, 449(7164), 890-U9, doi:10.1038/nature06227, 2007.

van Geen, A., Zheng, Y., Bernhard, J. M., Cannariato, K. G., Carriquiry, J., Dean, W. E., Eakins, B. W., Ortiz, J. D. and Pike, J.: On the preservation of laminated sediments along the western margin of North America, Paleoceanography, 18(4), doi:10.1029/2003pa000911, 2003.

Gómez-Valdivia, F., Parés-Sierra, A. and Flores-Morales, A. L.: The Mexican Coastal Current: A subsurface seasonal bridge that connects the tropical and subtropical Northeastern Pacific, Cont. Shelf Res., 110, 100–107, doi:10.1016/j.csr.2015.10.010, 2015.

Hain, M. P., Sigman, D. M. and Haug, G. H.: Shortcomings of the isolated abyssal reservoir model for deglacial radiocarbon changes in the mid-depth Indo-Pacific Ocean, Geophys. Res. Lett., 38, doi:10.1029/2010gl046158, 2011.

Herguera, J. C., Herbert, T., Kashgarian, M. and Charles, C.: Intermediate and deep water mass distribution in the Pacific during the Last Glacial Maximum inferred from oxygen and carbon stable isotopes, Quat. Sci. Rev., 29(9–10), 1228–1245, doi:10.1016/j.quascirev.2010.02.009, 2010.

Jaccard, S. L. and Galbraith, E. D.: Large climate-driven changes of oceanic oxygen concentrations during the last deglaciation, Nat. Geosci., 5(2), 151–156, doi:10.1038/ngeo1352, 2011.

698 Jaccard, S. L., Galbraith, E. D., Martínez-García, A. and Anderson, R. F.: Covariation of
699 deep Southern Ocean oxygenation and atmospheric CO2 through the last ice age,
700 Nature, 530(7589), 207–210, doi:10.1038/nature16514, 2016.

701 Keeling, C. D.: The concentration and isotopic abundances of carbon dioxide in the
702 atmosphere, Tellus, 12(2), 1960.

703 Keigwin, L. D.: Late Pleistocene-Holocene paleoceanography and ventilation of the
704 Gulf of California, J. Oceanogr., 58(2), 421–432, 2002.

705 Keigwin, L. D. and Guilderson, T. P.: Bioturbation artifacts in zero-age sediments,
706 Paleoceanography, 24(4), doi:10.1029/2008PA001727, 2009.

707 Keigwin, L. D. and Lehman, S. J.: Radiocarbon evidence for a possible abyssal front
708 near 3.1 km in the glacial equatorial Pacific Ocean, Earth Planet. Sci. Lett., 425, 93–
709 104, doi:10.1016/j.epsl.2015.05.025, 2015.

710 Key, R. M., Kozyr, A., Sabine, C. L., Lee, K., Wanninkhof, R., Bullister, J. L., Feely, R. A.,
711 Millero, F. J., Mordy, C. and Peng, T. H.: A global ocean carbon climatology: Results
712 from Global Data Analysis Project (GLODAP), Glob. Biogeochem. Cycles, 18(4),
713 doi:10.1029/2004gb002247, 2004.

714 Lindsay, C. M., Lehman, S. J., Marchitto, T. M. and Ortiz, J. D.: The surface expression
715 of radiocarbon anomalies near Baja California during deglaciation, Earth Planet. Sci.
716 Lett., 422, 67–74, doi:10.1016/j.epsl.2015.04.012, 2015.

717 Lindsay, C. M., Lehman, S. J., Marchitto, T. M., Carriquiry, J. D. and Ortiz, J. D.: New
718 constraints on deglacial marine radiocarbon anomalies from a depth transect near
719 Baja California, Paleoceanography, 31(8), 1103–1116, doi:10.1002/2015PA002878,
720 2016.

721 Lougheed, B. C., Metcalfe, B., Ninnemann, U. S. and Wacker, L.: Moving beyond the
722 age-depth model paradigm in deep sea palaeoclimate archives: dual radiocarbon
723 and stable isotope analysis on single foraminifera, Clim. Past Discuss., 1–16,
724 doi:10.5194/cp-2017-119, 2017.

725 Lund, D. C.: Deep Pacific ventilation ages during the last deglaciation: Evaluating the
726 influence of diffusive mixing and source region reservoir age, Earth Planet. Sci. Lett.,
727 381, 52–62, doi:10.1016/j.epsl.2013.08.032, 2013.

728 MacFarling Meure, C., Etheridge, D., Trudinger, C., Steele, P., Langenfelds, R., van
729 Ommen, T., Smith, A. and Elkins, J.: Law Dome CO2, CH4 and N2O ice core records
730 extended to 2000 years BP, Geophys. Res. Lett., 33(14), doi:10.1029/2006GL026152,
731 2006.

732 Magana, A. L., Southon, J. R., Kennett, J. P., Roark, E. B., Sarnthein, M. and Stott, L. D.:
733 Resolving the cause of large differences between deglacial benthic foraminifera

734 radiocarbon measurements in Santa Barbara Basin, Paleoceanography, 25(4),
735 doi:10.1029/2010PA002011, 2010.

736 Marchitto, T. M., Lehman, S. J., Ortiz, J. D., Fluckiger, J. and van Geen, A.: Marine
737 Radiocarbon Evidence for the Mechanism of Deglacial Atmospheric CO2 Rise,
738 Science, 316, 1456–1459, 2007.

739 Marcott, S. A. and Shakun, J. D.: A record of ice sheet demise, Science, 358(6364),
740 721–722, doi:10.1126/science.aaq1179, 2017.

741 Middleton, J. L., Langmuir, C. H., Mukhopadhyay, S., McManus, J. F. and Mitrovica, J.
742 X.: Hydrothermal iron flux variability following rapid sea level changes, Geophys.
743 Res. Lett., 43(8), 3848–3856, doi:10.1002/2016GL068408, 2016.

744 Monnin, E.: Atmospheric CO2 Concentrations over the Last Glacial Termination,
745 Science, 291(5501), 112–114, doi:10.1126/science.291.5501.112, 2001.

746 Petit, J. R., Jouzel, J., Raynaud, D., Barkov, N. I., Barnola, J. M., Basile, I., Bender, M.,
747 Chappellaz, J., Davis, M., Delaygue, G., Delmotte, M., Kotlyakov, V. M., Legrand, M.,
748 Lipenkov, V. Y., Lorius, C., Pepin, L., Ritz, C., Saltzman, E. and Stievenard, M.: Climate
749 and atmospheric history of the past 420,000 years from the Vostok ice core,
750 Antarctica, Nature, 399(6735), 429–436, 1999.

751 Reimer, P., Bard, E., Bayliss, A., Beck, J., Blackwell, P., Bronk, R., Buck, C., Cheng, H.,
752 Edwards, R., Friedrich, M., Grootes, P., Guilderson, T., Haflidason, H., Hajdas, I., Hatte,
753 C., Heaton, T., Hoffmann, D., Hogg, A., Hughen, K., Kaiser, K., Kromer, B., Manning, S.,
754 Niu, M., Reimer, R., Richards, D., Scott, E., Southon, J., Staff, R., Turney, C. and van der
755 Plicht, J.: IntCal13 and Marine13 radiocarbon age calibration curves 0–50,000 years
756 cal BP., Radiocarbon, 55(4), 1869–1887, 2013.

757 Roach, L. D., Charles, C. D., Field, D. B. and Guilderson, T. P.: Foraminiferal
758 radiocarbon record of northeast Pacific decadal subsurface variability, J. Geophys.
759 Res. Oceans, 118(9), 4317–4333, doi:10.1002/jgrc.20274, 2013.

760 Robinson, L. F., Adkins, J. F., Keigwin, L. D., Southon, J., Fernandez, D. P., Wang, S.-L.
761 and Scheirer, D. S.: Radiocarbon Variability in the Western North Atlantic During the
762 Last Deglaciation, Science, 310, 1469–1473, 2005.

763 Ronge, T. A., Tiedemann, R., Lamy, F., Köhler, P., Alloway, B. V., De Pol-Holz, R.,
764 Pahnke, K., Southon, J. and Wacker, L.: Radiocarbon constraints on the extent and
765 evolution of the South Pacific glacial carbon pool, Nat. Commun., 7, 11487,
766 doi:10.1038/ncomms11487, 2016.

767 Rose, K. A., Sikes, E. L., Guilderson, T. P., Shane, P., Hill, T. M., Zahn, R. and Spero, H. J.:
768 Upper-ocean-to-atmosphere radiocarbon offsets imply fast deglacial carbon dioxide
769 release, Nature, 466(7310), 1093–1097, doi:10.1038/nature09288, 2010.

Santos, G. M., Moore, R. B., Southon, J. R., Griffin, S., Hinger, E. and Zhang, D.: AMS 14C sample preparation at the KCCAMS/UCI Facility: status report and performance of small samples, Radiocarbon, 49(2), 255–270, 2007.

Sikes, E. L., Samson, C. R., Guilderson, T. P. and Howard, W. R.: Old radiocarbon ages in the southwest Pacific Ocean during the last glacial period and deglaciation, Nature, 405, 6, 2000.

Skinner, L. C., Fallon, S., Waelbroeck, C., Michel, E. and Barker, S.: Ventilation of the Deep Southern Ocean and Deglacial CO2 Rise, Science, 328(5982), 1147–1151, 2010.

Southon, J., Santos, G., Druffel-Rodriguez, K., Druffel, E., Trumbore, S., Xu, X., Griffin, S., Ali, S. and Mazon, M.: The Keck Carbon Cycle AMS laboratory, University of California, Irvine: initial operation and a background surprise, Radiocarbon [online] Available from: https://escholarship.org/uc/item/0xw7c8b3.pdf (Accessed 10 June 2016), 2004.

Stott, L. and Timmermann, A.: Hypothesized Link Between Glacial/Interglacial Atmospheric CO2 Cycles and Storage/Release of CO2-Rich Fluids From Deep-Sea Sediments, in Geophysical Monograph Series, vol. 193, edited by H. Rashid, L. Polyak, and E. Mosley-Thompson, pp. 123–138, American Geophysical Union, Washington, D. C., 2011.

Stott, L., Southon, J., Timmermann, A. and Koutavas, A.: Radiocarbon age anomaly at intermediate water depth in the Pacific Ocean during the last deglaciation, Paleoceanography, 24(2), doi:10.1029/2008PA001690, 2009.

Stuiver, M. and Polach, H. A.: Discussion; reporting of C-14 data., Radiocarbon, 19(3), 355–363, 1977.

Stuiver, M., Reimer, P. and Reimer, R.: CALIB 7.1. [online] Available from: http://calib.org (Accessed 2 January 2017), 2017.

Subhas, A. V., Adkins, J. F., Rollins, N. E., Naviaux, J., Erez, J. and Berelson, W. M.: Catalysis and chemical mechanisms of calcite dissolution in seawater, Proc. Natl. Acad. Sci., 114(31), 8175–8180, doi:10.1073/pnas.1703604114, 2017.

Thornalley, D. J. R., Barker, S., Broecker, W. S., Elderfield, H. and McCave, I. N.: The Deglacial Evolution of North Atlantic Deep Convection, Science, 331(6014), 202–205, doi:10.1126/science.1196812, 2011.

Thornalley, D. J. R., Bauch, H. A., Gebbie, G., Guo, W., Ziegler, M., Bernasconi, S. M., Barker, S., Skinner, L. C. and Yu, J.: A warm and poorly ventilated deep Arctic Mediterranean during the last glacial period, Science, 349(6249), 706–710, doi:10.1126/science.aaa9554, 2015.

805 Tolstoy, M.: Mid-ocean ridge eruptions as a climate valve, Geophys. Res. Lett., 42(5),
806 1346–1351, doi:10.1002/2014GL063015, 2015.

807 Voelker, A. H. L., Sarnthein, M., Grootes, P. M., Erlenkeuser, H., Laj, C., Mazaud, A.,
808 Nadeau, M.-J. and Schleicher, M.: Correlation of Marine 14C Ages from the Nordic
809 Seas with the GISP2 Isotope Record: Implications for 14C Calibration Beyond 25 ka
810 BP, Radiocarbon, 40(01), 517–534, doi:10.1017/S0033822200018397, 1998.

811 Wycech, J., Kelly, D. C. and Marcott, S.: Effects of seafloor diagenesis on planktic
812 foraminiferal radiocarbon ages, Geology, 44(7), 551–554, doi:10.1130/G37864.1,
813 2016.

814 Zhao, N. and Keigwin, L. D.: An atmospheric chronology for the glacial-deglacial
815 Eastern Equatorial Pacific, Nat. Commun., 9(1), doi:10.1038/s41467-018-05574-x,
816 2018.

817

818

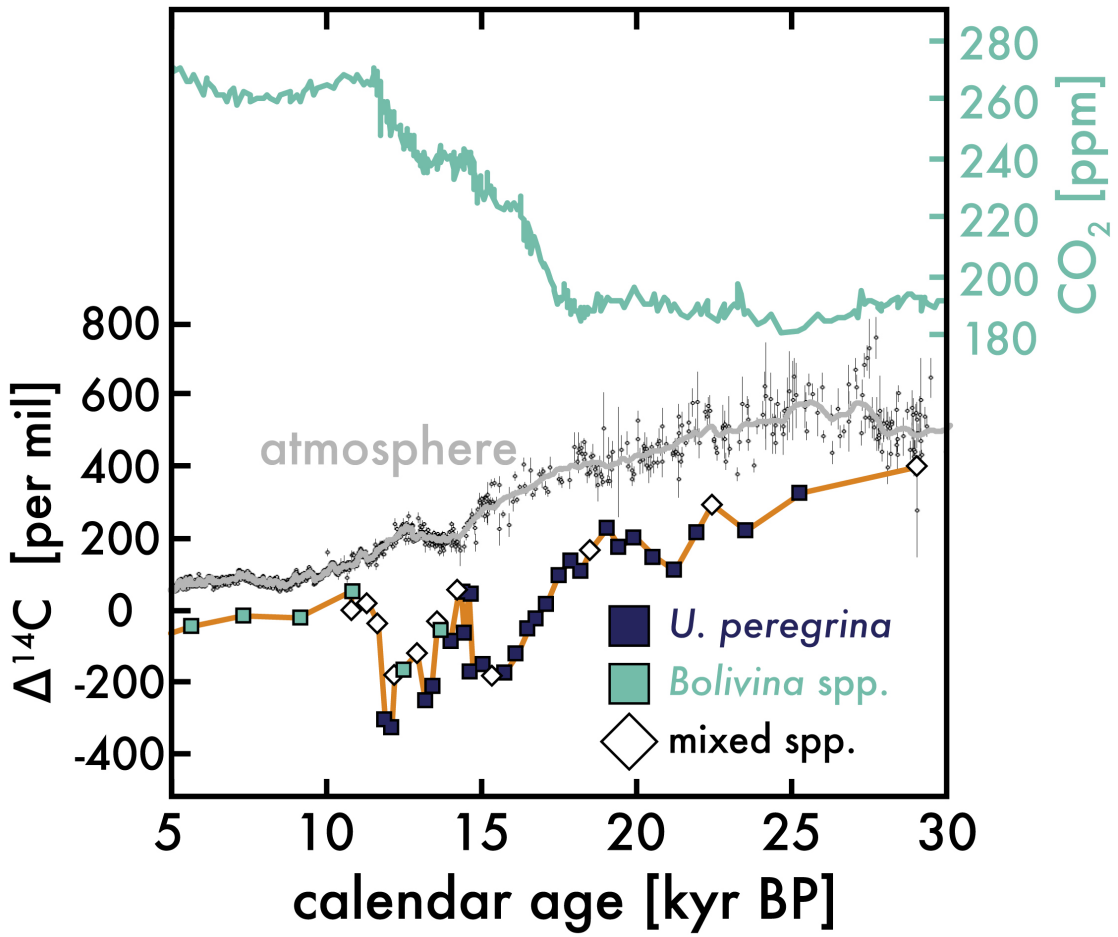

819
820 **Figure 1.** Atmospheric carbon dioxide (CO_2) concentrations (top; blue) (Ahn and
821 Brook, 2014; MacFarling Meure et al., 2006; Marcott and Shakun, 2017; Monnin,
822 2001), atmospheric $\Delta^{14}C$ (middle: blank symbols observations; gray line is
823 smoothed average) (Reimer et al., 2013), and benthic foraminifera $\Delta^{14}C$ from
824 sediment bathed in California Undercurrent water (orange; see Table 1 and maps in
825 Figure 2) (Lindsay et al., 2015; Marchitto et al., 2007). These observations are
826 shown from 30-to-5-kyr BP (BP = before 1950).
827
828

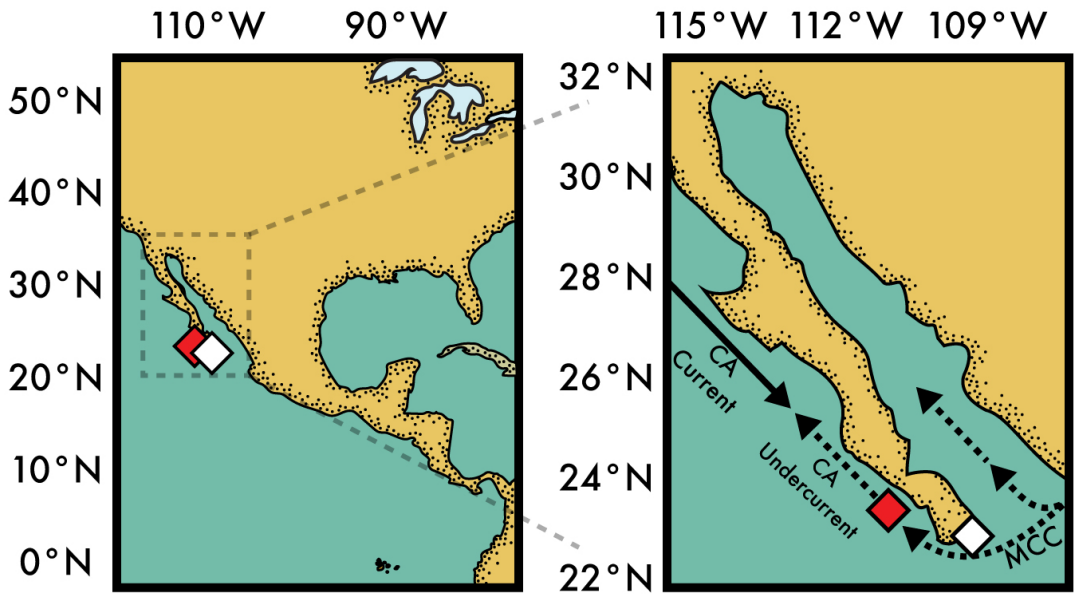

Figure 2. Maps of sediment core sites (diamonds; see Table 1) and ocean circulation (arrows: solid = surface; dashed = near seafloor). The foraminifera radiocarbon measurements in Figure 1 are from core sites at the red diamond (Marchitto et al., 2007; Lindsay et al., 2016). See Table 1 for details on site locations. Note that the subsurface Mexican Coastal Current (MCC) flows between 200 to ≈700 m and feeds subsurface water into both the Gulf of California and California Undercurrent (Gómez-Valdivia et al., 2015)—waters that bathe both core sites.

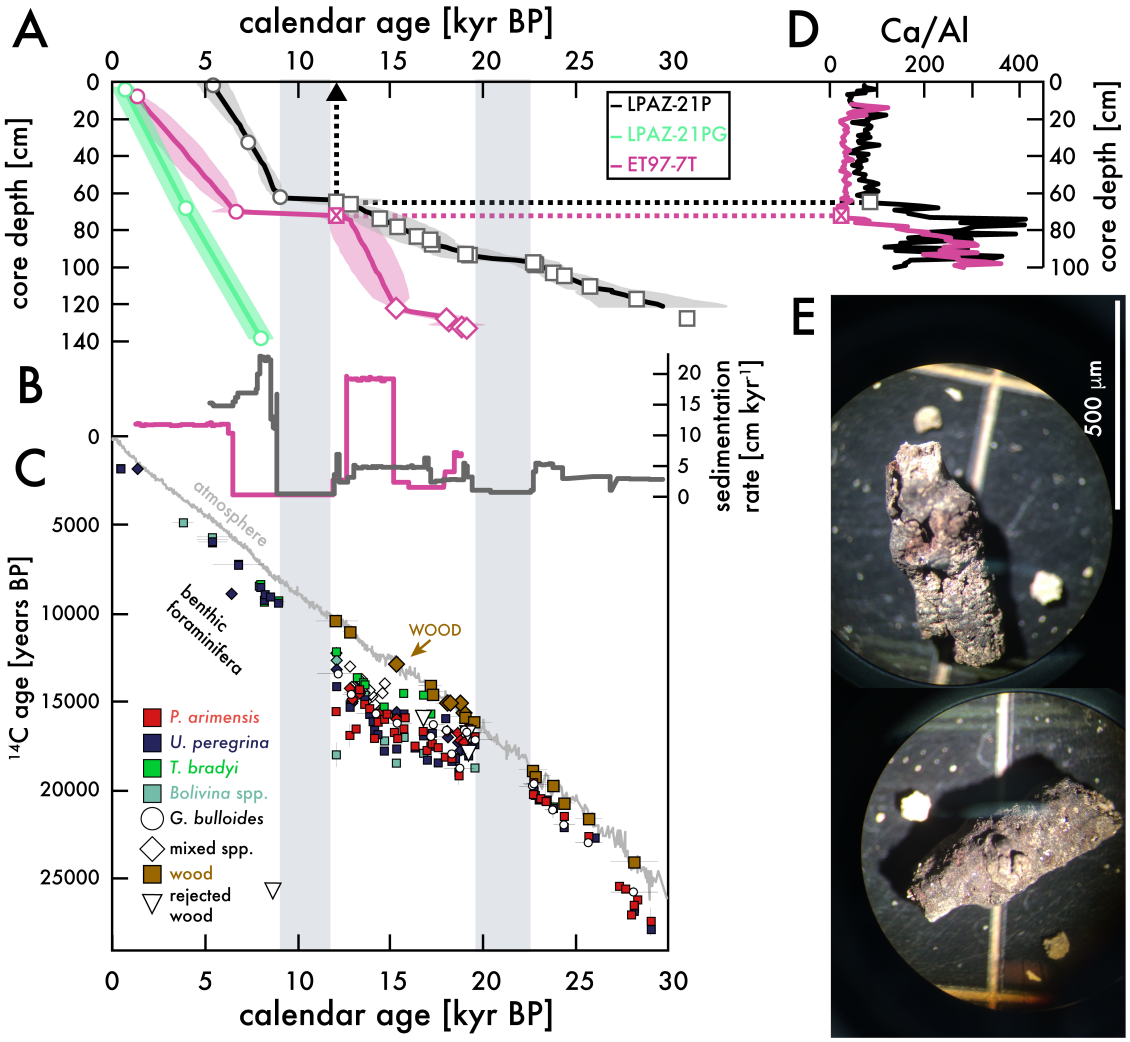

839

840 **Figure 3.** (A) Sediment core depth versus calendar age. Age model constraints are
841 based on wood ^{14}C (squares and diamonds), stratigraphic correlation ("X"; see (D)),
842 and U. peregrina ^{14}C corrected for reservoir age (circles). (B) Sedimentation rate
843 versus calendar age. (C) The ^{14}C age of atmospheric CO_2, foraminifera, wood, and
844 rejected wood (see legend) versus calendar age for ET97-7T (diamonds) and LPAZ-
845 21P/ LPAZ-21PG (squares). See Figure 1 and Table 1 for locations. (D) Ca/Al for
846 ET97-7T (pink) and LPAZ-21P (black) was measured using X-Ray Fluorescence (see
847 Methods). Lower Ca/Al for the uppermost sediment (beginning at the arrows) is
848 coincident with loss of calcium carbonate microfossils and an overall darkening of
849 sediments at these and other sites in the region (van Geen et al., 2003). We use this
850 stratigraphic feature to tie the age model for both sites (dashed arrow between
851 "X"s). (E) Examples of wood found within sediment core LPAZ-21P (see scale).

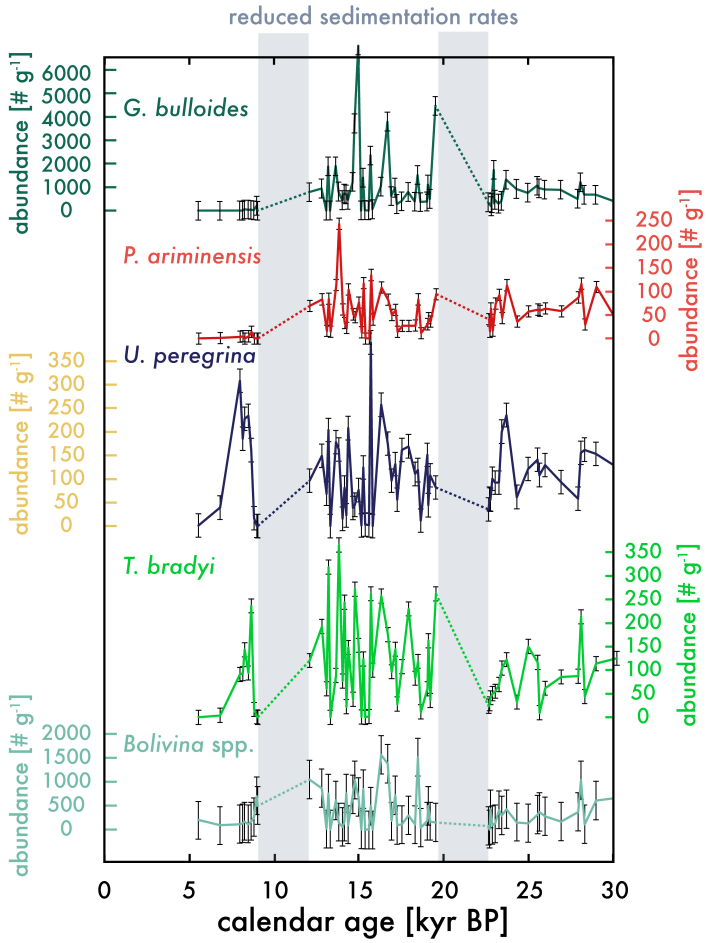

Figure 4. Foraminifera abundance at site LPAZ-21P for planktic (*G. bulloides*) and benthic species (all others). Error bars represent 2 times the typical standard deviation for replicate counts.

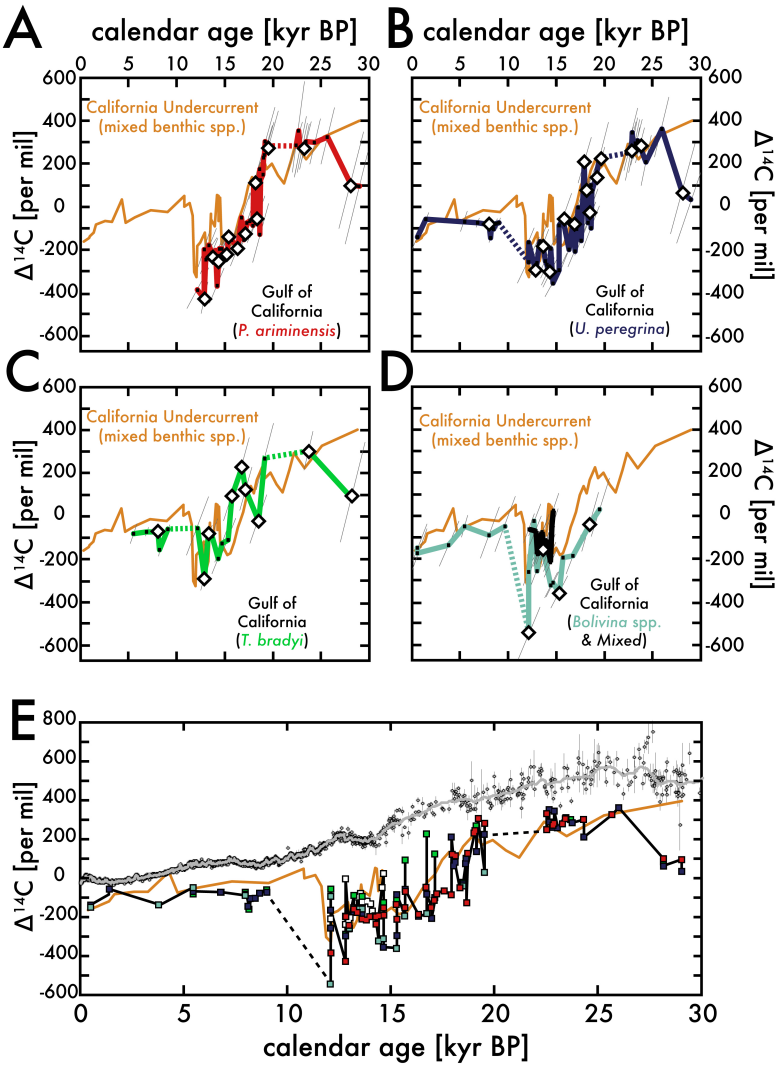

Figure 5. The ^{14}C isotopic composition (corrected for decay as $\Delta^{14}C$) for Gulf of California benthic foraminifera mono-species (A-D) and mixed species (D) are compared with mono- and mixed-species benthic foraminifera $\Delta^{14}C$ measurements from the California Undercurrent sediment core site (orange) (Lindsay et al., 2015; Marchitto et al., 2007) over the past 35,000 years BP. See core locations in Figure 2. Canted error bars take into account measurement and age model errors (Stuiver et al., 2017). Diamonds indicate $\Delta^{14}C$ at foraminifera abundance maximum. The $\Delta^{14}C$ of all Gulf benthic foraminifera (see Figure 3 legend) is shown in (E) alongside atmospheric $\Delta^{14}C$ (grey) (Reimer et al., 2013) and California Undercurrent site $\Delta^{14}C$ (orange). Modern $\Delta^{14}C$ near the depth of the Gulf and Pacific sites is about -173‰ (Key et al., 2004).

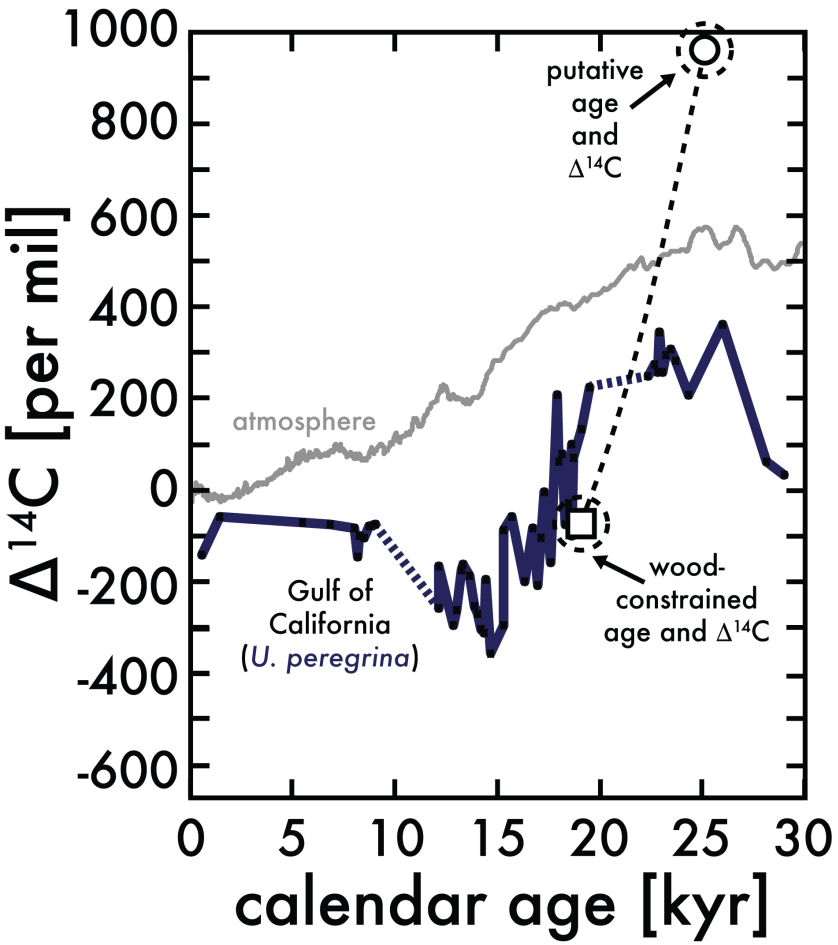

871

872 **Figure 6**: Comparing Gulf of California *U. peregrina* $\Delta^{14}C$ with anomalous values
873 based on the Bayesian calendar age (circle) based on sediment depth and the wood-
874 constrained calendar age (square). If this anomaly was not the result of human error
875 (mislabeling of the sample's depth), then this may suggest the influence of
876 macrofauna. See text for more details.

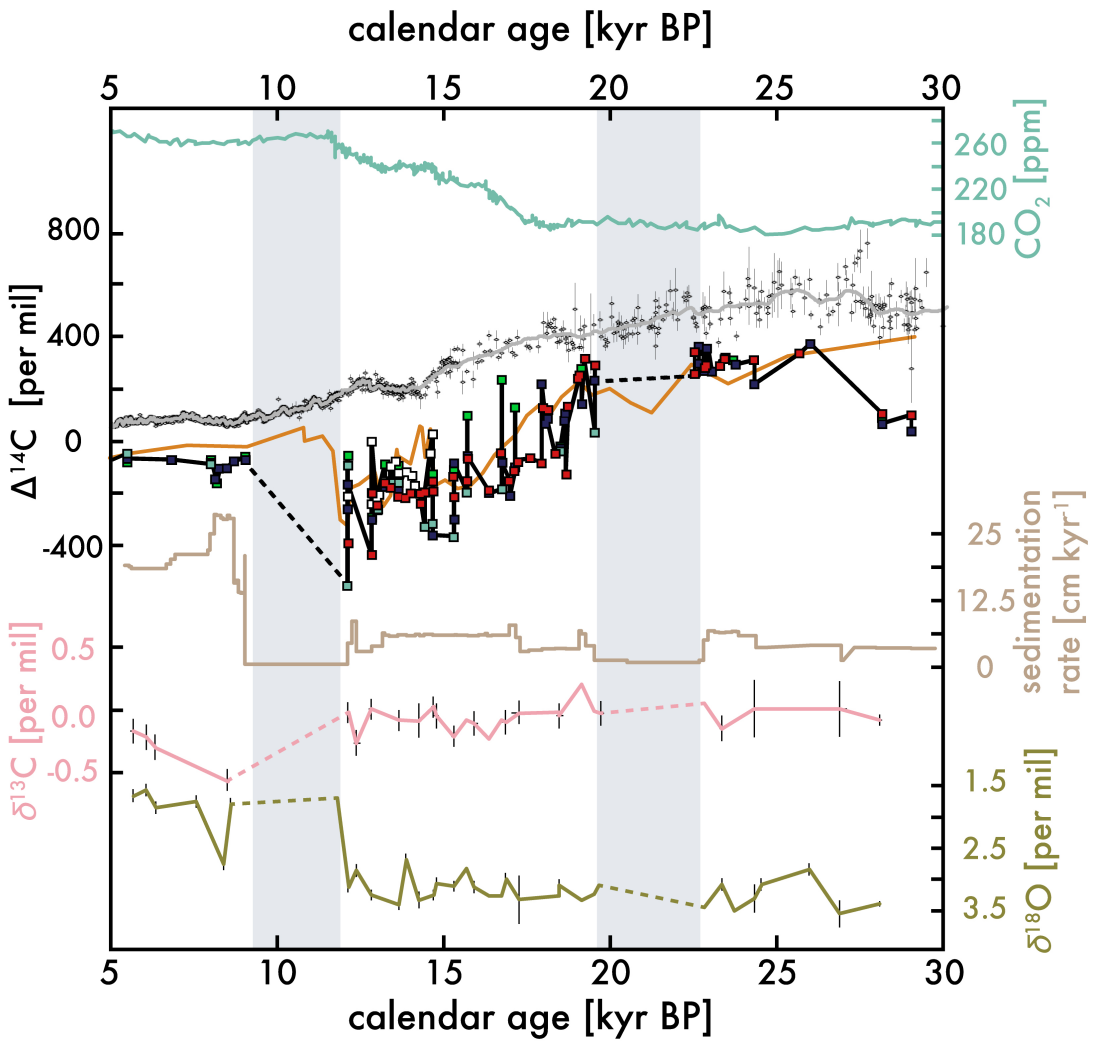

877

878 **Figure 7.** From top to bottom: atmospheric carbon dioxide (CO_2) (blue; same as
879 Figure 1), atmospheric CO_2 $\Delta^{14}C$ (grey; same as Figure 1), mixed and mono-species
880 benthic foraminifera $\Delta^{14}C$ from the California Undercurrent site (red) (Lindsay et al.,
881 2015; Marchitto et al., 2007), all mono-species benthic foraminifera $\Delta^{14}C$ from near
882 the mouth of the Gulf of California (black; this study), sedimentation rate of LPAZ-
883 21P (see Figure 3), benthic foraminifera *P. ariminensis* $\delta^{13}C$ (pink) and $\delta^{18}O$ (green)
884 from this study and Herguera et al., (2010).

885

886

887 **Table 1.** Latitude, longitude, depth below modern sea surface, and modern
888 dissolved inorganic carbon (DIC) $\Delta^{14}C$ (26) at the sediment-seawater interface for
889 sediment cores discussed in this study.

Table 1	latitude [°N]	longitude [°W]	depth [m]	modern DIC $\Delta^{14}C$ [‰] at this depth
LPAZ-21P / LPAZ-21PG	22.9	109.5	624	-148
ET97-7T	22.9	109.5	640	-148
MV99-MC19/GC31/PC08	23.5	111.6	705	-148

890
891 **Table 2.** The difference between benthic foraminifera and concurrent wood ^{14}C
892 ages for all measurements ("ALL") and only at abundance maxima (see Figure 4).
893

	The difference between *P. ariminensis* - wood [^{14}C years]		The difference between *U. peregrina* - wood [^{14}C years]	
	ALL	abundance maxima	ALL	abundance maxima
AVERAGE	2346	2488	2309	2697
STDEV	1599	1791	1063	1117
n	14	11	13	6

894

895 **Table 3.** Comparison between benthic foraminifera ^{14}C ages for all measurements
896 ("ALL") and only at abundance maxima (see Figure 4).
897

	The difference between *P. ariminensis* - *U. peregrina* [^{14}C years]		The difference between *P. ariminensis* - *T. bradyi* [^{14}C years]		The difference between *P. ariminensis* - *Bolivina* spp. [^{14}C years]	
	ALL	abundance maxima	ALL	abundance maxima	ALL	abundance maxima
AVERAGE	-104	10	826	35	-857	-1407
STDEV	759	861	1484	1125	939	597
n	42	8	7	4	11	2

898